International Journal of
INTELLIGENT SYSTEMS AND APPLICATIONS IN ENGINEERING
ISSN:2147-6799 www.ijisae.org Original Research Paper

Machine Learning Algorithms for Ocular Disease from Fundus Images using LBP and HOG

Santhosh Kumar B N[1], Dr. G N K Suresh Babu[2]

Submitted: 28/01/2024 **Revised**: 06/03/2024 **Accepted**: 14/03/2024

Abstract: Despite their diminutive size, eyes are essential to human life. Given the importance of the visual system among the four sense organs and the variety of eye disorders that might arise, it is imperative to identify abnormalities of the external eye as soon as possible. Severe visual impairment or blindness can result from ocular illness, a progressive eye disorder associated with diabetes. To diagnose and cure it, specialists use non-invasive images of the retina called fundus imaging. Expert knowledge and high-quality images are prerequisites for accurate picture classification. Eight distinct groups of ocular diseases that cause blindness were taken into consideration in the suggested effort. The dual-stage method for identifying ocular disorders described in this article uses the Histogram of Oriented Gradients (HOG) and local binary patterns (LBP) for feature extraction. Next, machine learning methods like support vector machines (SVM), random forests (RF), and K-Nearest Neighbours (KNN) are used for classification operations. This study contrasts eight methods for identifying eye diseases. The results show that the combination of HOG and SVM, with an accuracy of 92.2%, and LBP and SVM, with a combination of 98.1%, attained the maximum accuracy.

Keywords: *Fundus images, Histogram of Oriented Gradients, K-Nearest Neighbors, Local Binary Patterns, Ocular Disease, Random Forests.*

1. Introduction

Nearly 2.2 billion people are estimated to suffer vision impairment globally by the World Health Organisation (WHO), and at least 1 billion of these instances could have been avoided [1]. Over time, the prevalence of ocular illnesses has increased, and one reason for this tendency is the way that human behaviour has changed due to technological advancements and technology. Thus, ocular diseases have greatly impacted modern human lives. Among the common ailments that can lead to blindness include diabetes, glaucoma, hypertension, cataracts, pathological myopia, and other eye disorders. Early detection can help lessen the severity of eye disorders, even though they can have very dangerous side effects, including blindness [2]. Artificial intelligence (AI) is a broad subject of computer science that studies concepts, methods, tools, and application systems for replicating, extending, and increasing human intelligence in machines [3]. Machine learning (ML) is a branch of artificial intelligence (AI) that uses statistical techniques to build intelligent systems [4]. The intelligent system can use either a supervised or unsupervised approach to automatically learn and enhance its performance, such as accuracy, without having to be explicitly built. Deep learning (DL) [5] has demonstrated impressive outcomes in computer vision and natural language processing applications by employing advanced machine learning techniques. This success is mainly attributable to its extraordinary feature extraction and pattern recognition capabilities, which use many processing layers (artificial neurons) to learn representations of data with increasing degrees of abstraction and connect the input with a diagnostic output. This outstanding achievement has led to DL's employment in medical and healthcare-related tasks by many researchers; thus, DL is currently a powerful tool for intelligent illness screening, diagnosis, and therapy. DL has been used to thyroid classification from ultrasound imaging, COVID-19 detection from chest X-rays, and lung nodule staging and detection from computed tomography (CT) images. In the future, wearable technology and smart home appliances will be able to dynamically monitor personal health data, offering an abundance of information for medical diagnosis. Accurate personal health information can be used to forecast illness risk in a standardised and reliable way by modelling these data. Artificial intelligence monitors health parameters, offers medication reminders, gives precise advice on managing blood pressure and blood sugar, and delivers complete, lifecycle health services to the public in a high-quality, thoughtful, and efficient way [6].

It was discovered by researchers that the vascular systems of the human retina exhibit geometric multi-fractal properties that are complicated and have a hierarchical arrangement of exponents as opposed to a single fractal dimension. In their investigation, they did not attempt to classify retinal pictures as healthy or afflicted by

[1]*Research Scholar, Srishti College of Commerce and Management, Banashankari, Bengaluru, Affiliated to University of Mysore, India, 560085.*
[2]*Professor, Department of Computer Science, Srishti College of Commerce and Management, Banashankari, Bengaluru, Affiliated to University of Mysore, India, 560085.*

glaucoma, even though they saw multi-fractal behaviour [7]. Here, the authors concentrate on the use of image texture for precise glaucoma classification. They do this by utilising SVM-based classification of glaucomatous images using the Histogram of Oriented Gradients (HOG) feature descriptor for statistical feature extraction. They emphasise the significance of the HOG technique in feature extraction by using it for preprocessing original photos to enhance output quality [8]. The authors of the research stress that edges should be ignored when calculating Local Binary Pattern (LBP) codes for images because they add incorrect data and don't provide enough information. The extracted feature vector can then be used as input for machine-learning algorithms that classify images, such as Support Vector Machines (SVMs) or Extreme Learning Machines (ELMs) [9].

Researchers investigated the importance of early diagnosis in raising awareness and delivering effective medical care. Following a comprehensive review of the literature, they have shown that the use of Local Binary Pattern (LBP) in conjunction with Histogram of Oriented Gradients (HOG) yields more accurate feature extraction results than other methods. With the recent development of AI algorithms, unprecedented opportunities to solve some of the major problems associated with DR and other ocular disorders are being presented. For instance, trained on annotated fundus images, the diagnosis performance of the Inception-v3 system can match that of human specialists. Regretfully, the technological foundation has not been thoroughly investigated, despite the existence of multiple pertinent assessments within the community [10–11].

This research leverages LBP and HOG features with machine learning algorithms to detect ocular diseases from fundus images, showcasing advancements in medical image analysis. By integrating these techniques, the study offers a promising approach for accurate disease diagnosis and management, potentially enhancing patient care in ophthalmology. The utilization of LBP and HOG features underscores their effectiveness in extracting relevant information from fundus images for efficient disease classification.

2. Materials and Methods

The methodology involves using feature extraction techniques and applying various Machine Learning (ML) algorithms for Ocular Disease (OD) identification and classification. The below Figure 1 illustrates the key steps in this process: Dataset of fundus images, which includes both normal and OD cases are considered in the work. Further these images are undergone with resize, normalize, and enhanced in contrast to ensure consistency and improve the quality of the dataset. Here, LBP and HOG have been used to extract local texture features from each image, capturing relevant patterns and details. Dataset has been divided into two parts: a training set and a testing set with 70-30 ratio. Few ML algorithms for classification, such as KNN, Random Forest, and Support Vector Machines are Trained using the training dataset, allowing them to learn the relationships between the extracted LBP and HOG features and OD. This methodology combines LBP and HOG feature extraction with various ML algorithms to create an effective system for diabetic retinopathy detection, aiding in early diagnosis and treatment.

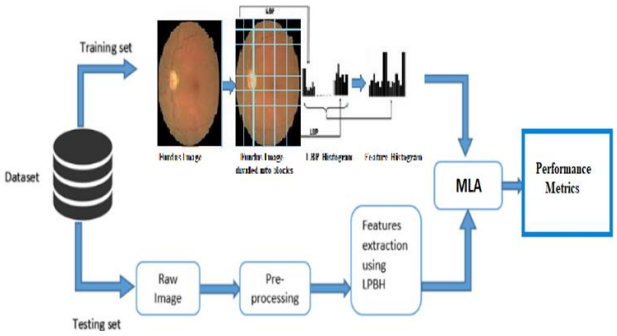

Figure 1: Ocular Disease detection using Machine Learning Algorithm

2.1 Local Binary Patterns Histogram (Lbph)

The initial Local Binary Patterns (LBP) operator was introduced by Ojala et al. (reference [12]). It acts on the eight neighbours that surround a pixel within a segmented unit known as a cell. Every pixel in the cell is compared to its eight neighbours. A binary code of one or zero is assigned to each pixel, depending on whether the neighbor's value is larger than or equal to the value of the centre pixel. These binary codes are then combined to create a decimal with 256 dimensions, which is used as the centre pixel's texture description [13]. In Figure 2, the original LBP operator is shown.

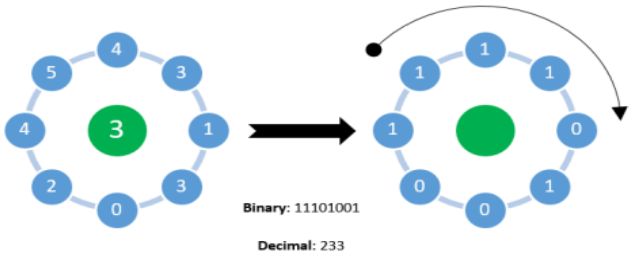

Figure 2: LBP Operator

Our suggested method requires feature reduction and effective fundus picture representation due to the resource-intensive nature of correlation algorithms [14]. Through the application of histograms, we were able to efficiently capture local patterns for dimensionality reduction, reducing the features from a 256-dimensional decimal to a condensed 59-dimensional histogram.Concatenating all of the regional histograms yields the global description of the fundus image. An histogram of the total value of LBPH looks like Figure 3:

$$LBP_{M,N} = \sum_{r=0}^{7} 2^r \, g(k_r - k_c) \quad (1)$$

$$g(a) = \begin{cases} 1 \; ; \; a \geq 0 \\ 0 \; ; \; a < 0 \end{cases} \quad (2)$$

$$H(k) = \sum \sum f(LBP_{M,N} \; g(a,b), k), k \, \varepsilon [0, K]$$

$$H(k) = \sum_{i=0}^{n} \sum_{j=1}^{m} f\left(LBP_{P,R}(i,j), k\right), k \in [0, k] \quad (3)$$

where P is the sampling points and R is the radius. Where k is the maximal LBP pattern value.

$$g(a,b) = \begin{cases} 1 \; ; \; a = b \\ 0 \; ; \; otherwise \end{cases} \quad (4)$$

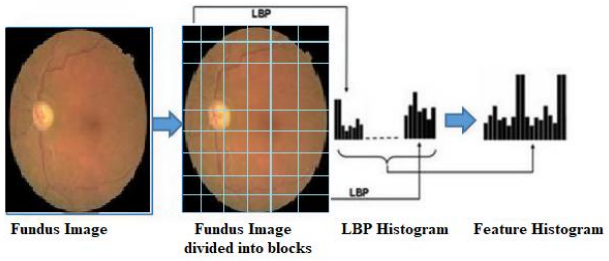

Figure 3: Feature Extraction using LBP

2.2 HOG

The Histogram of Oriented Gradients (HOG) feature extraction method is commonly applied in image processing, recording the frequency of gradient orientations within specific regions of an image. By dividing the image into small linked areas known as cells, a HOG descriptor is computed for pixels within each cell, utilizing gradient magnitude and angle calculations to quantify the image's texture and structure [15]. G_x and G_y is calculated using the formulae (5) for each pixel value.For each pixel (x,y) in the input image I thetwo-dimensional gradient G(x, y)=(Gx(x, y), Gy (x, y))is determined. The gradient magnitude |G(x, y)| and gradient angle φ(x, y) at position (x, y) are given by equation (6).

$$g = \sqrt{g_x^2 + g_y^2} \quad (5)$$

$$\tan \theta = \frac{g_y}{g_x} \quad (6)$$

where the gradients in the x and y directions are denoted by G_x and G_y, respectively. The gradient histogram is then computed. As in previous studies [17–16], the HOG descriptor was selected to describe the various forms of DR lesions. The total number of HOG characteristics that were extracted was examined for various sizes of HOG cells. Orientation binning, the third step, was carried out. Before moving on to the next step, the fourth stage computes normalisation, which takes local groups of cells and contrasts normalises their total responses [18]. The process of normalisation prepares the images for training. Equation (7) is then used to generate the final HOG feature vector, which can be utilised for both training and classification.

$$f = \frac{V}{\sqrt{||V_2^2|| + e^2}} \quad (7)$$

Where, V-descriptor vector, and ‘e’ represent small-value constants.

2.3 Classification

After extracting the features, the classification process is initiated using three classifiers, namely, KNN, SVM and RF. The computation procedures involved the utilization of fundus images sourced from database, serving as both the training and test datasets. This dataset comprises diverse manifestations of eye disorders, encompassing conditions like Cataracts, Diabetic Retinopathy, Glaucoma, and normal eye images for comprehensive analysis and model training as shown in Figure 4.

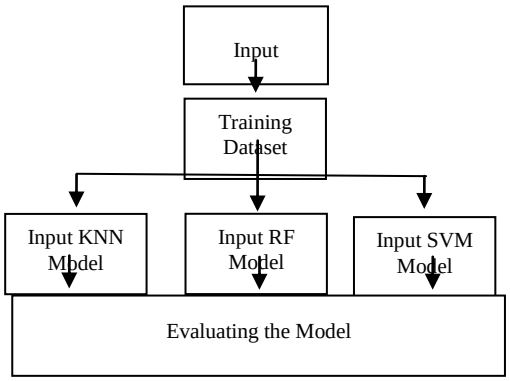

2.4 Support Vector Machine:

SVM is a kind of machine learning algorithm that recognises patterns and performs regression using the concepts of statistical learning and structural risk minimization. Finding the ideal hyperplane to maximally maximise the margin between positive and negative examples while successfully separating the former from the latter is the primary objective of support vector machines (SVM).SVM's benefit is its capacity to handle non-linear data and challenging classification issues. Additionally, because it maximises the margin between classes, it is resistant to overfitting [19]. Moreover, SVM is a widely used technique in pattern recognition due to its excellent classification accuracy. Because of its computational complexity, SVM is not ideal for processing very big data sets. Furthermore, appropriate parameter selection—such as C and gamma parameters—is necessary to achieve the best outcomes [20].

2.5 Random Forest Multiple decision trees are used in this strategy to create the categorization. To categorise eye photos, a random generator will create each tree [21]. The prediction class will be decided by these trees' majority judgement. RF is a machine learning technique that generates a final prediction by aggregating the predictions of several decision trees. A bootstrapping procedure results in the production of several trees, hence the title "Random Forest". Every tree in RF produces a class prediction of its own, and the most frequent forecast from the trees is chosen as the final prediction [22].Because of a special property, the RF algorithm can introduce more unpredictability into the tree-growth process. When splitting a node, RF uses a random selection of features to discover the optimal features, in contrast to other approaches that prioritise the most significant features. Significant diversity is introduced by this method, which frequently leads to improved model performance and more durable designs [23].

2.6 K-Nearest Neighbors (KNN)

For applications involving pattern recognition and predictive modelling, this algorithm offers a simple yet efficient non-parametric regression and classification technique. the nearest neighbours of a new data point, as determined by a majority vote or average, in the feature space; the "nearest" neighbours are determined using a distance metric. The key parameter in KNN, as shown in figure 5, represents the number of neighbours to be considered [24].Greater values of k provide choice borders that are smoother and more resilient to noise, but the underlying patterns may become overly simplistic. Less than optimal values of k lead to more intricate decision limits and heightened susceptibility to local variations in the data, which may cause overfitting.

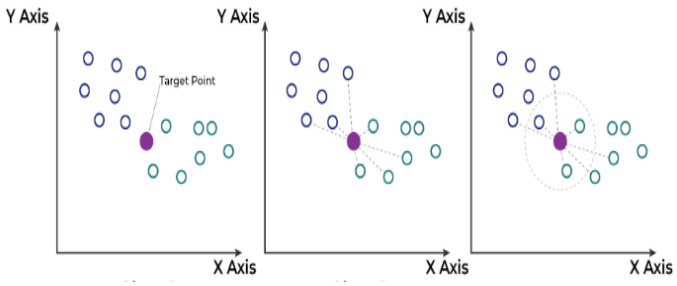

Figure 5:KNN for different Neighbours setting

To determine how unlike the features are from one another, various distance metrics such as Minkowski, Euclidean, and Seuclidean are employed. In KNN, the class label or value of a new point is often determined by the Euclidean distance [23–25].

3 Results and Discussions

The following steps provide an organized representation of the many phases of the research process.

Step 1: After pertinent data is acquired from reliable sources, preprocessing addresses any anomalies, missing values, or inconsistencies to ensure the data is ready for further analysis.

Step 2: Finding the crucial elements or traits from the pre-processed dataset that are required for the modelling stage is crucial. Using algorithms and statistical methodologies, this step uses LBP and HOG to separate the most significant characteristics for the subsequent training phase.

Step 3: It is essential for determining the significant variables or traits—required for the modelling stage—from the pre-processed dataset. In this step, algorithms and statistical techniques are used to separate the most significant features for the subsequent training phase utilising LBP and HOG.

Step 4: From the pre-processed dataset, it is essential for determining the significant variables or features required for the modelling phase. For the following training phase, this stage uses algorithms and statistical techniques to separate the most significant features using LBP and HOG.

For the computational procedures, we utilized eye images sourced from both Kaggle and the Medimrg database, serving as training and testing datasets. These datasets encompass a variety of eye disorders, including Cataracts, Diabetic Retinopathy, Glaucoma, and Normal cases. The original OCT images are sized at 512x512x3, but for feature extraction, they are resized to 224x224x3. A total of 6000 images were employed for experimentation. These images are categorized into Age-related Macular Degeneration (1), Hypertension (2), non-proliferate retinopathy (3), Pathological Myopia (4), Cataract (5), Diabetic Retinopathy (6), Glaucoma (7), and Normal (8). Among these, 70% of the data is allocated for training the model, while the remaining 30% is reserved for result verification and network accuracy assessment. The study computes and tabulates metrics such as True Positive Rate (TPR), False Positive Rate, and Accuracy. Two feature extraction techniques, Histogram of Oriented Gradients (HOG) and Local Binary Patterns (LBP), were applied to process fundus images for detecting ocular diseases. Following this, machine learning models including K-nearest neighbors (KNN), Random Forest, and Support Vector Machine (SVM) were developed to classify these images. The integration of LBP feature extraction with KNN, RF, and SVM classifiers facilitates comprehensive performance evaluation, aiding in the selection of the most appropriate classifier for accurate diagnosis and treatment planning in medical scenarios. The classification models were evaluated using 5-fold cross-validation to ensure robustness and generalization. Statistical analysis was performed on the cross-validated results to assess the

performance of each model, providing valuable insights into their efficacy for ocular disease diagnosis.

During each iteration, four subsets are used for training, and the remaining one is reserved for testing, ensuring comprehensive assessment, and reducing over fitting. Local Binary Patterns (LBP) feature extraction is employed to characterize image textures effectively, crucial in medical image analysis. Results corresponding to KNN algorithm classifies for individual sub classes in shown in Table 1 and its 5-fold cross validation results are tabulated in Table 2.The KNN algorithm achieved an overall accuracy of 93.4% and an AUC of 0.993, indicating strong discriminatory ability. Specifically, classes 2, 3, and 5 attained precision, recall, and F1-score values exceeding 98%, demonstrating excellent performance in correctly identifying instances from these classes.

Table 1: Performance metric for each Class using KNN

Class	Se	Sp	Prc	Recall	F1-	AUC	Acc
1	0.115	0.885	0.604	0.9	0.628	0.973	0.919
2	0.106	0.894	0.855	0.875	0.961	1	0.968
3	0.124	0.876	0.64	0.917	0.76	1	0.925
4	0.122	0.878	0.592	0.951	0.815	0.996	0.917
5	0.084	0.916	0.512	0.87	0.611	1	0.915
6	0.069	0.931	0.567	0.892	0.891	0.999	0.943
7	0.065	0.935	0.361	0.774	0.493	1	0.881
8	**0.062**	**0.938**	**0.336**	0.755	0.356	1	0.876

Table 2: 5-fold cross validation using KNN

Fold	Precision	Recall	F1-	AUC	Accuracy
1	0.838	0.835	0.913	0.996	0.959
2	0.601	0.915	0.868	0.973	0.933
3	0.729	0.724	0.685	0.996	0.931
4	0.773	0.394	0.365	0.999	0.891
5	0.859	0.790	0.824	1.000	0.954
Avg:	**0.760**	**0.732**	**0.731**	**0.993**	**0.934**

Random Forest (RF) constructs an ensemble of decision trees and combines their predictions through voting. Results corresponding to RF algorithm classifies for individual sub classes in shown in Table 3 and its 5-fold cross validation results are tabulated in Table 4.The Random Forest (RF) algorithm demonstrated an overall accuracy of 91.7% and an AUC of 0.993, indicative of strong discriminatory performance. Notably, class 2 achieved precision, recall, and F1-score values exceeding 96%, underscoring RF's proficiency in accurately identifying instances from this class while maintaining competitive performance across other metrics.

Table 3: Performance metric for each Class using RF

Class	Se	Sp	Prc	Recall	F1-	AUC	Acc
1	0.1	0.9	0.609	0.698	0.637	0.973	0.903
2	0.126	0.874	0.972	0.986	0.984	1	0.995
3	0.124	0.876	0.975	0.997	1.172	1	0.996
4	0.105	0.895	0.76	0.758	0.715	0.996	0.938
5	0.126	0.874	0.933	0.997	1.461	1	0.991
6	0.059	0.941	0.773	0.437	0.424	0.999	0.915
7	0.121	0.879	0.761	0.934	0.967	1	0.955
8	0.105	0.895	0.923	0.87	0.947	1	0.976

Table 4: 5-fold cross validation RF

Fold	Precision	Recall	F1	AUC	Accuracy
1	0.558	0.867	0.692	0.996	0.918
2	0.538	0.919	0.641	1	0.892
3	0.553	0.842	0.821	0.999	0.939
4	0.608	0.87	0.611	0.973	0.919
5	0.603	0.923	0.806	0.996	0.917
Avg:	**0.572**	**0.884**	**0.714**	**0.993**	**0.917**

Additionally, Support Vector Machine (SVM) finds the optimal hyperplane to separate different classes in the feature space. Results corresponding to SVM algorithm classifies for individual sub classes in shown in Table 5 and its 5-fold cross validation results are tabulated in Table 6.The Support Vector Machine (SVM) algorithm exhibited outstanding performance with an overall accuracy of 98.1% and an AUC of 0.999, indicative of excellent discriminatory capability. Notably, except for class 6, all other classes achieved accuracy values surpassing 90%, underscoring SVM's effectiveness as the best classifier for LBP features, particularly in accurately classifying instances across a diverse range of classes. These results emphasize SVM's robustness and suitability for precise classification tasks, highlighting its potential for reliable medical image analysis.

Table 5: Performance metric for each Classusing RF

Class	Se	Sp	Precision	Recall	F1-	AUC	Acc
1	0.095	0.905	0.601	0.915	0.598	0.973	0.933
2	0.114	0.886	0.862	0.975	0.893	1	0.979
3	0.12	0.88	0.914	0.968	0.963	1	0.985
4	0.126	0.874	0.885	0.953	0.963	0.996	0.978
5	0.122	0.878	0.901	0.957	1.477	1	0.981
6	0.067	0.933	0.773	0.394	0.358	0.999	0.891
7	0.085	0.915	0.875	0.824	0.874	1	0.971
8	0.112	0.888	0.859	0.79	0.808	1	0.954

The ROC curves in figure 6 and confusion matrix in figure 7 for KNN, RF, and SVM classifiers for LBP showcase their performance across various threshold values and provide insights into their ability to correctly classify instances. into their ability to correctly classify instances.

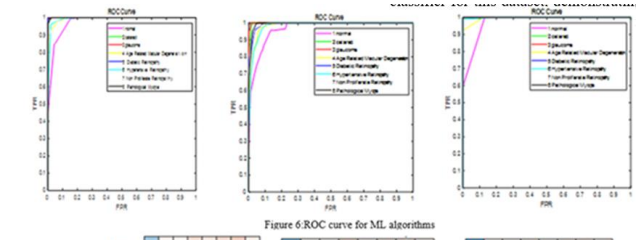

Figure 6:ROC curve for ML algorithms

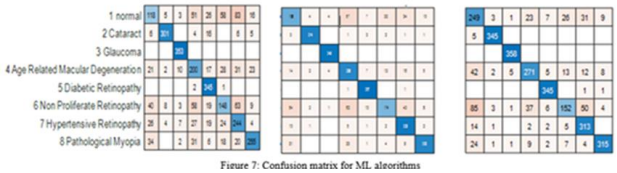

Fisure 7: Confusion matrix for ML algorithms

Table 6: 5-fold cross validation -SVM

Fold	Precision	Recall	F1-Score	AUC	Accuracy
1	0.862	0.975	0.855	1	0.979
2	0.885	0.953	0.912	0.996	0.978
3	0.914	0.968	0.962	1	0.985
4	0.914	0.968	0.963	1	0.985
5	0.868	0.985	0.999	1	0.98
Avg:	**0.888**	**0.97**	**0.938**	**0.999**	**0.981**

In a similar fashion HOG s feature extraction has been employed to process fundus images for ocular disease detection. Furthermore, the same machine learning models were developed to classify these images. A comparison of LBP and HOG on these ML models are analysed using statistical parameters and the same is tabulae in Table 7. When comparing the performance of KNN, RF, and SVM classifiers using LBP and HOG features, SVM

consistently achieves the highest accuracy across both feature types. Specifically, with LBP features, SVM attains an accuracy of 98.1%, outperforming KNN's 93.4% and RF's 91.7%. Similarly, with HOG features, SVM maintains its superiority with an accuracy of 92.2%, while KNN and RF achieve accuracies of 84.1% and 82.4%, respectively. These results suggest that SVM is the most effective classifier for this dataset, demonstrating its robustness and versatility in capturing underlying patterns, regardless of the feature representation used.

Table 7: Comparison of ML algorithms with LBP and HOG

	KNN		Random forest		SVM	
	LBP	HOG	LBP	HOG	LBP	HOG
Precision	0.76	0.634	0.572	0.526	0.888	0.835
Recall	0.732	0.659	0.884	0.796	0.97	0.912
F1-Score	0.731	0.658	0.714	0.643	0.938	0.882
AUC	0.993	0.894	0.993	0.894	0.999	0.939
Accuracy	0.934	0.841	0.917	0.824	0.981	0.922

Conclusion

To predict multiple eye disease, this study suggested an efficient OCT classification system based on the proposed model. experiments to categorise OCT into different classes using the kaggle dataset. The OCT scans tend to vary more considerably amongst patients as the number of patients with disease is found. In conclusion, In comparing KNN, RF, and SVM classifiers using both LBP and HOG features, SVM consistently achieves the highest accuracy across both feature sets. Specifically, with LBP features, SVM achieves 98.1% accuracy, surpassing KNN at 93.4% and RF at 91.7%. Similarly, with HOG features, SVM

maintains its superiority with 92.2% accuracy, while KNN and RF achieve 84.1% and 82.4% accuracy, respectively. These findings underscore SVM's effectiveness in accurately classifying the dataset, showcasing its adaptability and robustness across different feature representations. These results highlight the promising prospects of utilizing the LBP-SVM combination to advance early diagnosis and management of ocular diseases from fundus images. By providing a valuable tool for healthcare professionals, this approach has the potential to enhance patient outcomes within the field of ophthalmology, paving the way for improved diagnostic accuracy and timely interventions.

References

[1] Ouda, Osama, Eman AbdelMaksoud, A. A. Abd El-Aziz, and Mohammed Elmogy. "Multiple ocular disease diagnosis using fundus images based on multi-label deep learning classification." Electronics 11, no. 13 (2022): 1966.

[2] Shi, Yuqi, Nan Jiang, Priyanka Bikkannavar, M. Francesca Cordeiro, and Ali K. Yetisen. "Ophthalmic sensing technologies for ocular disease diagnostics." Analyst 146, no. 21 (2021): 6416-6444.

[3] Sheng, Bin, Xiaosi Chen, Tingyao Li, Tianxing Ma, Yang Yang, Lei Bi, and Xinyuan Zhang. "An overview of artificial intelligence in diabetic retinopathy and other ocular diseases." Frontiers in Public Health 10 (2022): 971943.

[4] Tamhane, Mitalee, Sara Cabrera-Ghayouri, Grigor Abelian, and Veena Viswanath. "Review of biomarkers in ocular matrices: challenges and opportunities." Pharmaceutical research 36, no. 3 (2019): 40.

[5] U. R. Acharya, N. Kannathal, E. Y. K. Ng, L. C. Min,and J. S. Suri, “Computer-based classification of eye diseases,” in 2006 International Conference of the IEEEEngineering in Medicine and Biology Society, 2006, pp.6121–6124.

[6] Kumar, Yogesh, and Surbhi Gupta. "Deep transfer learning approaches to predict glaucoma, cataract, choroidal neovascularization, diabetic macular edema, drusen and healthy eyes: an experimental review." Archives of Computational Methods in Engineering 30, no. 1 (2023): 521-541.

[7] McCarthy J, Minsky ML, Rochester N, Shannon CE. A proposal for the dartmouth summer research project on artificial intelligence. AI Mag. (2006) 27:12. doi: 10.1007/978-1-4613-8716-9

[8] Samuel AL. Some studies in machine learning using the game of checkers. II—recent progress. Comput Games I. (1988) 1:366–400. doi: 10.1007/978-1-4613-8716-9_15

[9] Sanghavi, Jignyasa, and Manish Kurhekar. "Ocular disease detection systems based on fundus images: a survey." Multimedia Tools and Applications (2023): 1-26.

[10] LeCun Y, Bengio Y, Hinton G. Deep learning. Nature. (2015) 521:436–44. doi: 10.1038/nature14539PubMed

[11] Lee CS, Tyring AJ, Deruyter NP, Wu Y, Rokem A, Lee AY. Deep-learning based, automated segmentation of macular edema in optical coherence tomography. Biomed Opt Express. (2017) 8:3440–8. doi: 10.1364/BOE.8.003440

[12] Born J, Beymer D, Rajan D, Coy A, Mukherjee VV, Manica M, et al. On the role of artificial intelligence in medical imaging of COVID-19. Patterns. (2021) 2:100269. doi: 10.1016/j.patter.2021.100269

[13] Junayed, Masum Shah, Md Baharul Islam, Arezoo Sadeghzadeh, and Saimunur Rahman. "CataractNet: An automated cataract detection system using deep learning for fundus images." IEEE Access 9 (2021): 128799-128808.

[14] Chi J, Walia E, Babyn P, Wang J, Groot G, Eramian M. Thyroid nodule classification in ultrasound images by fine-tuning deep convolutional neural network. J Digit Imaging. (2017) 30:477–86. doi: 10.1007/s10278-017-9997-y

[15] Song J, Chai YJ, Masuoka H, Park SW, Kim SJ, Choi JY, et al. Ultrasound image analysis using deep learning algorithm for the diagnosis of thyroid nodules. Medicine. (2019) 98:e15133. doi: 10.1097/MD.0000000000015133.

[16] Malik, Sadaf, Nadia Kanwal, Mamoona Naveed Asghar, Mohammad Ali A. Sadiq, Irfan Karamat, and Martin Fleury. "Data driven approach for eye disease classification with machine learning." Applied Sciences 9, no. 14 (2019): 2789.

[17] Junayed, Masum Shah, Md Baharul Islam, Arezoo Sadeghzadeh, and Saimunur Rahman. "CataractNet: An automated cataract detection system using deep learning for fundus images." IEEE Access 9 (2021): 128799-128808.

[18] Setio AA, Ciompi F, Litjens G, Gerke P, Jacobs C, van Riel SJ, et al. Pulmonary nodule detection in CT images: false positive reduction using multi-view convolutional networks. IEEE Trans Med Imaging. (2016) 35:1160–9. doi: 10.1109/TMI.2016.2536809

[19] Hessen, Michelle, and Esen KaramurselAkpek. "Dry eye: an inflammatory ocular disease." Journal of ophthalmic & vision research 9, no. 2 (2014): 240.

[20] Sarki, Rubina, Khandakar Ahmed, Hua Wang, and Yanchun Zhang. "Automated detection of mild and multi-class diabetic eye diseases using deep learning." Health Information Science and Systems 8, no. 1 (2020): 32.

[21] Machan, Carolyn M., Patricia K. Hrynchak, and Elizabeth L. Irving. "Age-related cataract is associated with type 2 diabetes and statin use." Optometry and vision science 89, no. 8 (2012): 1165-1171.

[22] Ding J, Li A, Hu L Z, Wang. Accurate pulmonary nodule detection in computed tomography images using deep convolutional neural networks. In: Descoteaux M, Maier-Hein L, Franz A, Jannin P, Collins D, Duchesne S, , editors. Lecture Notes in Computer Science. Cham: Springer. (2017). p. 559–67.

[23] T. Ojala, M. Pietikäinen, and D. Harwood, ‘‘A comparative study of texture measures with classification based on featured distributions,’’ Pattern Recognit, vol. 29, no. 1, pp. 51–59, 1996.

[24] Nagaraju, C., and S. S. ParthaSarathy. “Embedding patient information in medical images using LBP and LTP.”Circuits and Systems: An International Journal 1, no. 1 (2014): 39-48.

[25] Sarki, Rubina, Khandakar Ahmed, Hua Wang, and Yanchun Zhang. "Automated detection of mild and multi-class diabetic eye diseases using deep learning." Health Information Science and Systems 8, no. 1 (2020): 32.